This study investigates the process of water jet motion in the air; the subject is the trajectory of motion and the velocity vector of water droplets in a two-phase "droplets-air" flow. The task addressed is to construct a model of water jet motion in the air, which would take into account its destruction and transformation into a stream of droplets.

A model of water jet motion in the field of gravity after exiting the fire hydrant in the area of the jet core has been built. The jet expansion coefficient was experimentally determined to be 0.016. Estimates of the jet radius, water droplet velocity, and effective radius of the jet of trapped air at the boundary of the core zone and the droplet zone were constructed. The values obtained are the initial conditions for the model of the motion of the droplet and gas phases of the jet in the droplet zone. The droplet motion was modeled by using the Lagrangian approach, within which the dynamics of the motion of individual drops were considered, described by the equations of motion in three-dimensional space taking into account the forces of aerodynamic resistance and gravity. It was assumed that the distribution of the droplet diameter obeys the Rosin-Ramler law.

A model of the motion of the gas phase of the jet was constructed, based on the equations of mass and momentum balance; it also takes into account the curvature of the jet axis due to the capture of air by drops moving under the action of gravity. The model is based on the assumption of the axisymmetric nature of the jet and the Gaussian velocity distribution in its cross section. A feature of the model is the mutual influence of the droplet and gas phases of the jet on the motion of each other: drops, losing momentum due to aerodynamic resistance, give it to the air. It is shown that drops of smaller diameter have a shorter range compared to drops of larger diameter. As a result, the water falls to the ground not at a specific point but in a certain range. In particular, for a fire hose with a diameter of 19 mm, a delivery angle of 35° to the horizon and a water pressure of (40÷70) m, the width of the range into which 90% of the water falls was (8.7÷11.0) m

Keywords: two-phase jet, drop zone, fire hose, jet core

UDC 614.84
DOI: 10.15587/1729-4061.2025.341606

BUILDING A MODEL OF WATER JET MOTION EXITING A FIRE HOSE

Oleksii Basmanov
Corresponding author
Doctor of Technical Sciences, Professor,
Leading Researcher
Scientific and Testing Department of Fire Protection and Fire Extinguishing Systems Research
Scientific and Research Center of Research and Testing
Institute of Scientific Research on Civil Protection**
E-mail: basmanov_oleksii@nuczu.edu.ua
Volodymyr Oliinyk
Doctor of Technical Sciences, Associate Professor,
Head of Department*
Oleh Zemlianskyi
Doctor of Technical Sciences, Professor,
Deputy Head of Department*
Olexander Derevyanko
PhD, Associate Professor*
Daryna Karpova
Lecturer
Department of Engineering and Technical Measures for Civil Protection**
*Department of Automatic Safety Systems and Electrical Installations**
**National University of Civil Protection of Ukraine
Onoprienka str., 8, Cherkasy, Ukraine, 18034

Received 04.08.2025
Received in revised form 03.10.2025
Accepted 14.10.2025
Published 28.10.2025

How to Cite: *Basmanov, O., Oliinyk, V., Zemlianskyi, O., Derevyanko, O., Karpova, D. (2025). Building a model of water jet motion exiting a fire hose. Eastern-European Journal of Enterprise Technologies, 5 (10 (137)), 77–86. https://doi.org/10.15587/1729-4061.2025.341606*

1. Introduction

Fires pose a serious threat to public safety, causing significant material damage and human casualties [1]. It is estimated that annual economic losses from fires worldwide reach billions of dollars, including the destruction of property, infrastructure, and restoration costs. In addition, fires have a significant environmental impact, in particular through emissions of carbon dioxide, toxic substances, and the destruction of natural ecosystems, which contributes to climate change and biodiversity loss. Despite the spread of foam and powder fire extinguishing agents, water remains the main extinguishing agent. The efficiency of its delivery to the fire source directly affects the speed of localization and elimination of the fire. This is of particular importance for automated fire extinguishing systems and fire robots, where it is necessary to select water supply parameters without human intervention [2]. Automated systems are applied in situations where the arrival of fire departments is associated with a critical loss of time or human participation in firefighting carries additional risks to their health.

Therefore, it is a relevant task to conduct studies aimed at designing automated water supply systems for firefighting.

2. Literature review and problem statement

Existing methods for building a water jet trajectory model can be divided into two types: the application of mathematical modeling methods and the use of neural networks. The conventional approach to modeling the trajectory of water jets in firefighting is based on classical ballistic models that take into account gravity and air resistance [3]. However, due to interaction with air, the water jet loses its continuity, turning into a stream of drops [4]. This leads to a different nature of the interaction of the droplet stream with air compared to a continuous jet and, in particular, different air resistance. As a result, there is a deviation of the observed trajectories from the calculated

ones. In particular, it was noted in work [5] that ballistic models in which air resistance is assumed to be proportional to the speed of the jet give an overestimated range compared to the experiment. To correct this error, a method for compensating for the prediction of the jet range was proposed in the work. In [6], the ballistic model is corrected by additional parameters that are determined experimentally.

The main difficulty in the practical application of such models is that empirically selected parameter values give good agreement between calculated and experimental data only under the conditions for which these values were selected. Another consequence of the destruction of a continuous jet is that different drops have different trajectories, different ranges, and different transverse deviations. As a result, classical ballistic models can give only the average range of the jet. Therefore, there is a need to use more complex models that take into account the motion of individual drops.

In [7], the disintegration of a circular liquid jet on a drop in still air was experimentally investigated. In this case, a weakly turbulent disintegration regime was observed (at low Weber and Reynolds numbers at the jet outlet), a turbulent disintegration regime (at moderate Weber numbers), and an aerodynamic shear disintegration regime (at high Weber numbers). However, the study concerned only jets falling vertically downwards. For horizontal jets, or jets directed at an angle to the horizon, the jet behavior changes due to different directions of the velocity vector and the gravity vector.

In [8], the disintegration of a water jet in air depending on the water pressure was investigated under laboratory conditions. However, the results were obtained for a nozzle with a diameter of 0.6 mm and their transfer to the case of fire hoses, the typical diameter of which is (19 ÷ 25) mm, is complicated.

In [9], the interaction of a horizontal water jet with air was experimentally investigated using a high-speed video camera. It was found that the jet expands with increasing distance to the nozzle. It was concluded that pressure is an important parameter that has an impact on the cluster and surface characteristics of the jet. However, such an important parameter for fire extinguishing as the delivery range was not considered in the work.

In [10], experimental data on the disintegration of jets were summarized and the disintegration modes were determined depending on the values of the criterion numbers of the jet, in particular the Weber number.

In [11], a model of the water jet motion was constructed, which takes into account the section of the continuous jet and the section of the droplet flow. However, the motion of the drops is considered in still air, although in reality the surrounding air is captured by the droplet flow, as a result of which the aerodynamic resistance decreases. A more accurate approach requires taking into account the motion of the gas phase of the jet.

In [12], a model of the water jet trajectory was constructed based on the Moving Particle Semi-implicit method. It was found that at low initial jet velocity the simulation results agreed well with the experimental data, while at high velocity significant errors were observed. It was found that the main cause of the deviation was air resistance. This result also indicates the need to take into account the movement of entrained air.

Another factor that affects the range of the jet is the size of the droplets formed. Droplets of smaller diameter are slowed down faster and therefore have a shorter range. In [13], the size of the droplets formed during the spraying of a water jet was experimentally investigated using high-speed imaging, and it was noted that their diameter can be described by the Rosin-Rammler distribution. It was concluded that the average diameter of the droplets is related to the Weber number of the jet and the geometry of the barrel.

The distribution of the size of the droplets formed during the spraying of a water jet was considered in detail in [14]. It was noted that the Rosin-Rammler law or the lognormal law can be used to describe this distribution. However, the issues of the motion of droplets in the air and the range of the jet are not considered in the cited works.

In [15], the motion of a water jet when it is supplied by a horizontally located fire hydrant with a diameter of 13 mm was experimentally investigated. The size and velocity of the droplets into which the continuous jet breaks up were determined. But the trajectory of the droplets was ignored, because.

In [16], a model of the water jet motion was constructed, which takes into account its breakdown into droplets and the further motion of the droplet flow. The proposed model is based on a one-dimensional Euler approach to the trajectory of the air flow and a Lagrangian approach to the trajectories of individual water droplets. This allowed the authors to take into account the entrainment of the surrounding air by the droplets, but the distribution of the droplets over the range was not considered in the work.

Instead of the approach that assumes a stationary distribution of velocities in the gas phase of the flow, a number of works use a general approach to modeling the motion of the air flow. In [17], for modeling a liquid jet in a supersonic flow, the motion of the gas phase is described using the Navier-Stokes equation system. This significantly complicates both calculations and generalization of the obtained results. In [18], the use of a high-speed water jet (300 ÷ 600 m/s) for extinguishing a gas flame was experimentally investigated.

In [19], a neural network was used to predict the jet drop point. The proposed approach takes into account both the jet parameters at the exit of the fire hydrant and the environmental parameters.

In [20], the Random Forest method was used to predict the jet drop point under random wind conditions. The disadvantage of such models is that they are tied to the data set on which the training was conducted. This leads to difficulties when applying them under other conditions.

In [21], a neural network was applied to compare the target and actual jet drop points with subsequent adjustment of the water supply parameters. This approach is advisable to use to increase the accuracy in automated water supply systems, but its application is impossible at the design stage.

All this gives grounds to argue that it is advisable to conduct research aimed at building a model of water jet movement in the air, which would take into account its destruction and transformation into a stream of drops.

3. The aim and objectives of the study

The aim of our work is to build a model of the movement of a water jet in the air after exiting the fire hose depending on the diameter of the nozzle, its angle of inclination, and water pressure. In practice, this opens up opportunities for the optimal selection of water supply parameters to the fire site or to protect objects in the zone of its thermal impact. This, in turn, makes it possible to improve the efficiency of fire extinguishing.

To achieve this aim, the following objectives were accomplished:

– to determine the characteristics of movement of a continuous water jet after exiting the fire hose;

– to construct the equation of motion for the drop phase of the jet;

– to construct the equation of motion for the gas phase of the jet.

4. The study materials and methods

The object of our study is the process of water jet motion in air; the subject of research is the trajectory of motion and the velocity vector of water droplets in a two-phase "droplet-air" flow. The principal hypothesis of the study assumes that the motion of a two-phase flow can be described as the motion of individual water droplets interacting with a gas jet, which arises as a result of the capture of ambient air by a water jet. The basic assumptions are the axisymmetric nature of the gas phase of the jet, the Gaussian velocity distribution in the cross-section of the jet, and the absence of secondary crushing or merging of droplets.

A fire hydrant with a nozzle diameter of (13 ÷ 25) mm was considered for supplying a continuous jet of water at a water pressure of (20 ÷ 80) m. To determine the trajectory of the water jet in the area of the jet core, the equation of motion of a material point in a gravitational field was applied. To model the motion of the droplet phase of the jet, the Lagrangian approach was used, within the framework of which the dynamics of individual drops were considered, described by the equations of motion in three-dimensional space taking into account the forces of aerodynamic resistance and gravity. The dynamics of the motion of the gas phase of the jet were described by the integral equations of mass and momentum balance. The Runge-Kutta method of the 4th order was used to numerically solve the system of differential equations of motion of the droplet and gas phases of the jet. Simulation modeling methods were used to study the trajectories of water droplets and the range of water supply from the fire hydrant. These methods were implemented in the Delphi 12 programming environment (USA).

5. Results of the construction of a model of water jet motion in air

5. 1. Determining the characteristics of motion of a continuous water jet after exiting a fire hose

The behavior of a water jet after exiting a fire hose is determined by the Weber number

$$We = \frac{\rho_\ell v_0^2 D_0}{\sigma}, \quad (1)$$

where v_0 is the initial jet velocity; D_0 is the diameter of the nozzle; ρ_ℓ is the density of water; σ is the coefficient of surface tension of water. The velocity of the water jet at the exit of the fire hose is related to the pressure by the following ratio

$$\frac{v_0^2}{2} = gh, \quad (2)$$

where h is the head; g is the acceleration of gravity. Substituting (2) into (1) gives

$$We = \frac{2\rho_\ell g h D_0}{\sigma}. \quad (3)$$

For typical values of the diameter of the fire hydrant nozzle (13 ÷ 25 mm) and the head (20 ÷ 80 m), expression (3) produced the value of the Weber number in the range of $7.1 \cdot 10^4 \div 5.4 \cdot 10^5$. At such values, the jet breaks up in the shear breakup regime [8]. This means that the jet begins to break up almost immediately after exiting the fire hydrant. The breakup occurs by exfoliation of individual drops (Fig. 1), as a result of which a conical jet core is formed (Fig. 2).

Fig. 1. Loss of continuity by a water jet when moving in the air (barrel nozzle diameter 19 mm, water pressure 70 m)

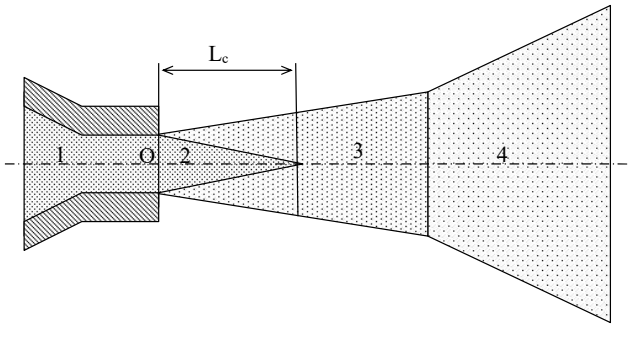

Fig. 2. Structure of a water jet in the air: 1 – water in a fire hose; 2 – jet core; 3 – water droplet zone; 4 – high diffused water droplet zone

For the specified range of Weber number values, the jet core length L_c is described by the following dependence [7]

$$\frac{L_c}{D_0} = 11.0\left(\frac{\rho_\ell}{\rho_a}\right)^{0.5}, \quad (4)$$

where ρ_a is the air density. For fire hoses with a nozzle diameter of (13÷25) mm, dependence (4) produced the length of the jet core

$$L_c \approx 314 D_0, \quad (5)$$

which corresponds to (4.1 ÷ 7.9) m provided $We > 3 \cdot 10^4$.

The detachment of individual drops leads to a visual expansion of the jet

$$R_w = \frac{D_0}{2} + c_w \ell\,, \tag{6}$$

where R_w is the radius of the jet at a distance ℓ from the barrel; c_w is an empirical coefficient that takes into account the expansion of the jet in the core zone and the drop zone. The value of this coefficient under the conditions of our full-scale experiment (Fig. 1) was 0.016.

Droplets that have separated from the jet core move not separately, but together, capturing the accompanying air. This leads to a decrease in air resistance and the preservation of visual continuity by the jet. In this case, the average droplet velocity v_s is close to the jet core velocity v [7]

$$v_s = 0.89v. \tag{7}$$

In view of the above, when building the model, it was assumed:

– in the core area (Fig. 2) the jet motion is determined by the initial velocity vector and the gravitational force;

– in the droplet zone (Fig. 2) the motion of a two-phase jet occurs, consisting of water droplets and entrained air;

– in the final section of the jet trajectory (high diffusion zone, Fig. 2) air entrainment does not occur, and each drop moves separately under the influence of gravitational force and air resistance.

In the core area, the jet motion can be described by a system of equations

$$\begin{cases} \dfrac{d^2x}{dt^2} = 0; \\ \dfrac{d^2z}{dt^2} = -g, \end{cases} \tag{8}$$

where the Z axis is directed vertically, the direction of the horizontal X axis coincides with the direction of the jet, and the origin of coordinates is at the exit from the barrel at point O (Fig. 2). Integration of system (8) produced

$$\begin{cases} x(t) = v_0 t\cos\theta; \\ z(t) = v_0 t\sin\theta - \dfrac{gt^2}{2}, \end{cases} \tag{9}$$

where θ is the angle between the fire hose and the horizontal surface. Neglecting the curvature of the jet allowed us to find the coordinates of the end point of the jet core from the following expression

$$v_0 t = L_c. \tag{10}$$

Substituting (10) into (9) gave the coordinates of the end point of the jet core (x_c, z_c) in the form

$$\begin{cases} x_c = L_c\cos\theta; \\ z_c = L_c\sin\theta - \dfrac{gL_c^2}{2v_0^2}. \end{cases} \tag{11}$$

At this point, the velocity vector (v_{xc}, v_{zc}) of the jet core is equal to

$$\begin{cases} v_{xc} = v_0\cos\theta; \\ v_{zc} = v_0\sin\theta - \dfrac{gL_c}{v_0}. \end{cases} \tag{12}$$

From (6) it follows that the radius of the water jet R_{w0} at this point

$$R_{w0} = \frac{D_0}{2} + c_w L_c. \tag{13}$$

Substituting (5) into (13) produced

$$R_{w0} = \frac{D_0}{2} + 314c_w D_0 = \left(0.5 + 314c_w\right)D_0 \approx 5.0D_0. \tag{14}$$

To determine the local velocity (u_x, u_y, u_z) of the entrained air at a certain point of the jet cross section, it was assumed that the velocity distribution is Gaussian depending on distance r to the jet axis

$$u(r) = u_c \exp\left(-\frac{r^2}{b_0^2}\right), \tag{15}$$

where b_0 is the effective radius of the jet, the value of which was determined from the condition that the average air velocity in the droplet zone is equal to its average velocity (7)

$$\frac{1}{S}\iint_S u(r)\,\mathrm{d}S = 0.89u_c, \tag{16}$$

where S is the cross section of the droplet zone of the jet at point (x_c, z_c)

$$S = \pi R_{w0}^2. \tag{17}$$

Combining expressions (15) to (17) produces:

$$\frac{b_0^2}{R_{w0}^2}\left(1 - \exp\left(-\frac{R_{w0}^2}{b_0^2}\right)\right) = 0.89;$$

$$\frac{R_{w0}^2}{b_0^2} \approx 0.2378;$$

$$b_0 = 2.051R_{w0}. \tag{18}$$

Substituting (14) into (18) gave the estimate

$$b_0 = 10.3D_0, \tag{19}$$

provided that the diameter of the fire hose nozzle $D_0 = (13\div25)$ mm.

5. 2. Construction of equations of motion for the drop phase of the jet

The end of the section with the jet core is the beginning of the drop zone (Fig. 2). The simulation of the drop phase of the jet was carried out by determining the trajectories of N individual drops. The size of the drops is related to the diameter of the fire hose nozzle by the following dependence

$$d_{32} = kD_0, \tag{20}$$

where the proportionality coefficient k is determined by the fluid motion regime [10]; d_{32} is the Sauter diameter

$$d_{32} = \frac{\sum_{i=1}^{N} d_i^3}{\sum_{i=1}^{N} d_i^2}; \quad (21)$$

d_i – diameter of the i-th drop. The proportionality coefficient for fire hoses is $k \approx 0.11$ [14].

The Rosin-Rammler law was used to describe the distribution of droplet diameters in the flow [22]

$$F(d) = 1 - \exp\left[-\left(\frac{d}{d_m}\right)^n\right], \quad (22)$$

where $F(d)$ is the fraction of the total volume contained in droplets with a diameter smaller than d; d_m is the representative diameter of the drop; n is the scattering measure. The representative diameter of the droplets d_m is related to the Sauter diameter by the following relation

$$d_m = d_{32}\frac{\Gamma\left(1+3/n\right)}{\Gamma\left(1+1/n\right)}, \quad (23)$$

where $\Gamma(x)$ is the gamma function. For fire hoses, the characteristic value of the scattering measure is $n = 3.0 \div 4.0$. In particular, from the histogram of droplet diameters given in [14], it follows that $n \approx 3.8$. Taking this into account, combining (20) and (23) gives

$$d_m = 0.113 D_0. \quad (24)$$

The initial coordinates of the drops were taken as

$$\begin{cases} x_i(0) = x_c; \\ y_i(0) = r_i \cos\phi_i; \\ z_i(0) = z_c + r_i \sin\phi_i, \end{cases} \quad (25)$$

where r_i, φ_i are realizations of random variables distributed uniformly on the intervals [0; R_{w0}] and [0; 2π], respectively. The initial velocity vector of the drop was chosen taking into account (7)

$$\begin{cases} v_{ix}(0) = 0.89 v_{xc}; \\ v_{iy}(0) = v_{ri} \cos\psi_i; \\ v_{iz}(0) = 0.89 v_{zc} + v_{ri} \sin\psi_i, \end{cases} \quad (26)$$

where v_{ri} is the radial velocity of the drop; v_{ri}, ψ_i are realizations of random variables distributed uniformly on the segments [0; $v_{r\max}$] and [0; 2π], respectively

$$v_{r\max} = \frac{R_{w0}}{t} = v_0 \frac{R_{w0}}{L_c}; \quad (27)$$

t is the time it takes for water to travel the distance from the barrel to the end of the jet core. Substituting (5) and (14) into (27) gives

$$v_{r\max} = 0.016 v_0.$$

The motion of a spherical drop in the air is determined by the influence of gravity and aerodynamic air resistance and can be described by a system of equations

$$\begin{cases} m_i \frac{dv_{ix}}{dt} = -\frac{1}{2}\rho_a C_D A_i w_i w_{ix}; \\ m_i \frac{dv_{iy}}{dt} = -\frac{1}{2}\rho_a C_D A_i w_i w_{iy}; \\ m_i \frac{dv_{iz}}{dt} = -m_i g - \frac{1}{2}\rho_a C_D A_i w_i w_{iz}, \end{cases} \quad (28)$$

where ρ_a is the air density; m_i, A_i are the mass and cross-sectional area of the i-th drop, respectively; (v_{ix}, v_{iy}, v_{iz}) is the vector of the droplet velocity in a fixed coordinate system, the center of which coincides with the fire hose; (w_{ix}, w_{iy}, w_{iz}) is the droplet velocity relative to the surrounding air:

$$\begin{cases} w_{ix} = v_{ix} - u_x; \\ w_{iy} = v_{iy}; \\ w_{iz} = v_{iz} - u_z; \end{cases} \quad (29)$$

$$w_i = \sqrt{w_{ix}^2 + w_{iy}^2 + w_{iz}^2};$$

(u_x, 0, u_z) is the velocity vector of the gas phase of the jet at a given point; C_D is the drag coefficient

$$C_D = \begin{cases} \frac{24}{\mathrm{Re}}\left(1 + 0.15\,\mathrm{Re}^{0.687}\right); \mathrm{Re} < 10^5; \\ 0.44; \mathrm{Re} \geq 10^5; \end{cases}$$

Re – Reynolds number

$$\mathrm{Re} = \frac{w_i d_i}{\nu_a};$$

ν_a is the kinematic viscosity of air. For a spherical drop with diameter d_i, the mass and cross-sectional area

$$m_i = \rho_\ell \frac{\pi d_i^3}{6}; \quad (30)$$

$$A_i = \frac{\pi d_i^2}{4}; \quad (31)$$

ρ_ℓ is the density of water. Substituting (30) and (31) into (28) gave the system of differential equations

$$\begin{cases} \frac{dv_{ix}}{dt} = -\frac{3}{4}\frac{\rho_a}{\rho_\ell} C_D \frac{1}{d_i} w_i w_{ix}; \\ \frac{dv_{iy}}{dt} = -\frac{3}{4}\frac{\rho_a}{\rho_\ell} C_D \frac{1}{d_i} w_i w_{iy}; \\ \frac{dv_{iz}}{dt} = -g - \frac{3}{4}\frac{\rho_a}{\rho_\ell} C_D \frac{1}{d_i} w_i w_{iz}. \end{cases} \quad (32)$$

The system of differential equations (32) together with the initial conditions (25), (26) determine the motion of water droplets in the droplet and high-diffusion zones (Fig. 2).

5. 3. Construction of equations of motion for the gas phase of the jet

The simulation of the motion of the gas phase of the jet was carried out under the assumption that it retains its axisymmetric nature. This allowed us to consider it in coordinates (s, r), where the s axis is directed along the jet axis,

and its origin coincides with the point (x_c, 0, z_c); r is the radial coordinate. It was assumed that the velocity profile of the gas phase retains a Gaussian character

$$u(s,r)=u_m(s)\exp\left(-\frac{r^2}{b^2(s)}\right), \quad (33)$$

where $u_m(s)$, $b(s)$ are the axial velocity and effective radius of the jet at point s, respectively. In this case, the horizontal and vertical components of the velocity of the gas phase of the jet are:

$$u_x=u(s,r)\cos\psi;$$

$$u_z=u(s,r)\sin\psi.$$

The mass and momentum balance equations for the gas phase of the jet are as follows:

$$\frac{d}{ds}\left(\pi b^2 u_m\rho_a\right)=2\pi b\alpha u_m\rho_a; \quad (34)$$

$$\frac{d}{ds}\left(\pi b^2 u_m^2\rho_a\right)=f, \quad (35)$$

where α is the entrainment coefficient of neighboring air masses. For circular jets $\alpha\approx 0.05$; f is the total reaction forces per unit length from all droplets arising from the deceleration or acceleration of droplets relative to the gas phase in the direction of the s axis

$$f(s)=\frac{1}{\Delta s}\sum_{i\in P(s)}F_{is}; \quad (36)$$

$P(s)$ – set of drops located in the cross section of the jet with a thickness of Δs, drawn through point s at a distance not exceeding $2b(s)$ from the jet axis; F_{is} – reaction force of the i-th drop in the direction of the s axis

$$F_{is}=F_{ix}\cos\psi+F_{iz}\sin\psi=$$
$$=\frac{\pi}{8}C_D\rho_a d_i^2 w_i\left(w_{ix}\cos\psi+w_{iz}\sin\psi\right). \quad (37)$$

Differentiation of the left-hand sides of equations (34), (35) and their combined transformation gave a system of ordinary differential equations for $u_m(s)$ and $b(s)$:

$$\frac{du_m}{ds}=\frac{f}{\pi b^2 u_m\rho_a}-\frac{2\alpha u_m}{b}; \quad (38)$$

$$\frac{db}{ds}=-\frac{f}{2\pi b u_m^2\rho_a}+2\alpha. \quad (39)$$

The movement of water droplets under the influence of gravity causes a force that distorts the axis of the jet:

$$\frac{d\psi}{ds}=-\frac{f_z\cos\psi}{\pi b^2 u_m^2\rho_a}; \quad (40)$$

$$f_z(s)=\frac{1}{\Delta s}\sum_{i\in P(s)}F_{iz}.$$

The coordinates of the gas phase axis of the jet are described by the differential equations

$$\frac{dx}{ds}=\cos\psi(s); \quad (41)$$

$$\frac{dz}{ds}=\sin\psi(s). \quad (42)$$

The combined solution of equations (38) to (42) under initial conditions:

$$b(0)=b_0=10.3D_0; \quad (43)$$

$$u_m(0)=\sqrt{v_{xc}^2+v_{zc}^2}=\sqrt{v_0^2-2gL_c\sin\theta+\left(\frac{gL_c}{v_0}\right)^2}; \quad (44)$$

$$\psi(0)=\operatorname{arctg}\frac{v_{zc}}{v_{xc}}=\operatorname{arctg}\left(\operatorname{tg}\theta-\frac{gL_c}{v_0^2\cos\theta}\right); \quad (45)$$

$$x(0)=x_c;\ \ z(0)=z_c, \quad (46)$$

determines the motion of the gas phase of the jet.

Fig. 3 shows the trajectories of water droplets of different diameters at the initial jet velocity $v_0=28$ m/s (barrel nozzle diameter $D_0=19$ mm, head $h=40$ m, barrel inclination angle $\theta=45°$).

Fig. 4 shows characteristics of the gas phase jet motion for the same conditions as in Fig. 3.

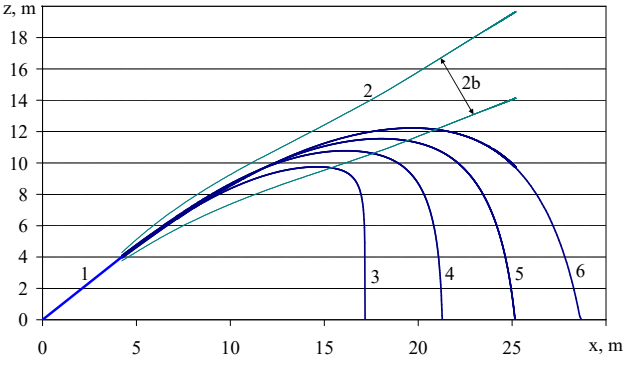

Fig. 3. Trajectory of the water jet after exiting the fire hose: 1 – core zone; 2 – boundaries of the gas phase of the jet in the drop zone; 3 – trajectory of a drop with a diameter of 0.84 mm; 4 – a drop of 1.56 mm; 5 – a drop of 2.23 mm; 6 – a drop of 2.93 mm

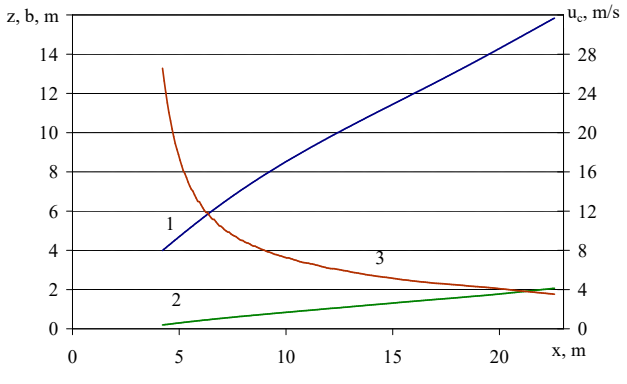

Fig. 4. Change in the characteristics of the gas phase of the jet movement depending on the distance to the fire hose: 1 – z-coordinate of the jet axis; 2 – effective radius; 3 – axial velocity (along the right axis)

Fig. 5 shows the effect of head on the distance of water supply by a fire hydrant with nozzle diameter $D_0 = 19$ mm, located at an angle of 35° to the horizon. To construct the density functions, a simulation of the motion of $3 \cdot 10^5$ individual drops was carried out.

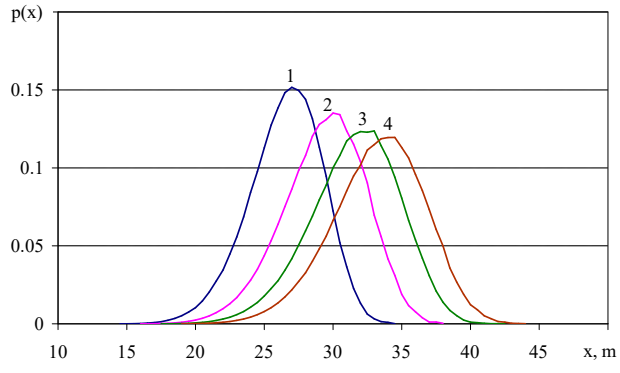

Fig. 5. Density function of the distribution of water supply distance depending on head: 1 – $h = 40$ m; 2 – $h = 50$ m; 3 – $h = 60$ m; 4 – $h = 70$ m

Analysis of the graphical relationships shown in Fig. 5 reveals that the range density function has a bell-shaped shape, but with some asymmetry. An increase in head at a constant angle of delivery leads to an increase in the average range with a simultaneous increase in the variance of distribution.

6. Results of the construction of a model of water jet motion in air: discussion

The behavior of a water jet after exiting a fire hydrant is determined by the Weber number (1). At a head of (20 ÷ 80) m, typical for fire hydrants, the initial velocity of the jet is in the range (19.8 ÷ 39.6) m/s. Taking into account the diameter of the nozzle of the hydrant (13 ÷ 25) mm, this corresponds to the values of the Weber number in the range $7.1 \cdot 10^4 \div 5.4 \cdot 10^5$. Such values of the Weber number mean that immediately after exiting the fire hydrant, the destruction of the continuous jet occurs due to the detachment of individual drops from its surface (Fig. 1). As a result, the continuous part of the jet acquires a conical shape (Fig. 2, jet core zone). The length of this section for the specified range of Weber number values depends only on the diameter of the fire hose nozzle and is determined from formula (4), which gives (4.1 ÷ 7.9) m. The loss of the vertical component of the velocity by the jet core occurs due to the action of gravity, and the horizontal component remains unchanged: a system of differential equations (8). Solving it (9) allows us to determine the coordinates of the end of the jet core (11) and its velocity vector (12) at this point.

Droplets that have separated from the core of the jet form a cone-shaped stream that expands with increasing distance from the fire hydrant (Fig. 2). Visually, this looks like the expansion of the jet (Fig. 1). Photofixation of the jet and subsequent measurement of the dependence of its width on the distance to the fire hydrant allowed us to estimate the expansion coefficient for the core zone and the drop zone. In particular, at the beginning of the drop zone, the radius of the water jet is described by dependence (14), which corresponds to values in the range (6.5 ÷ 12.5) cm for typical fire hydrants.

Study [7] notes that in the core zone, the average velocity of drops that have separated from the core is related to the velocity of the core via dependence (7). Together with formula (12), this allowed us to estimate the initial velocity of drops in the drop zone. Braking of separated drops by air leads to the transfer of the momentum of the drops to the air and its capture by the jet. As a result, in the drop zone the flow consists of two phases – drop and gas. The movement of the gas phase in the direction of the drop movement reduces the resistance force and extends the jet range. It was assumed that for the gas phase of the jet the velocity distribution depending on the distance to the jet axis has a Gaussian character (15). Together with the assumption that the average velocity of the gas phase coincides with the average velocity of the drops in the region (14), that made it possible to determine the effective radius of the gas phase of the jet at the beginning of the drop zone – formula (18). Its analysis reveals that the initial effective radius of the gas phase of the jet is approximately 2 times larger than the apparent radius of the water jet.

The motion of the droplet phase of the jet was modeled using a Lagrangian approach, which considered the dynamics of individual drops, described by the equations of motion in three-dimensional space taking into account the forces of aerodynamic resistance and gravity. The Rosin-Rammler law (22) was used to describe the distribution of droplet diameters. The representative droplet diameter included in (22) was estimated through its relationship with the Sauter diameter (21), which, in turn, is related to the diameter of the fire hydrant nozzle by relationship (20). This allowed us to obtain the dependence of the representative droplet diameter on the diameter of the fire hydrant nozzle in the form of (24). The measure of dispersion of droplet diameters included in the Rosin-Rammler law was determined based on the results reported in [14], in which drops from a fire hydrant with a nozzle diameter of 13 mm were experimentally investigated.

For each droplet, the initial coordinates (25) and the velocity vector (26) were randomly generated. The distribution parameters (25) were chosen so that the initial coordinates corresponded to the position of the droplet in the jet cross-section at the beginning of the droplet zone. In this case, the component of the velocity vector in the direction of the jet axis is equal to the average velocity of the drops at the beginning of the droplet zone. The transverse component was chosen so as to lead to a visual expansion of the water jet in accordance with (6).

The motion of a spherical droplet in the air, taking into account the forces of gravity and aerodynamic resistance, is described by a system of ordinary differential equations (28). After substituting the expressions for the mass of the droplet (30) and its cross-sectional area (31), the system of equations of motion of the droplet took the form of (32). For the numerical solution of the system of equations (32) under the initial conditions (25) and (26), the 4th-order Runge-Kutta method was used.

A feature of the system of equations (32) is that it includes the velocities of droplets relative to air. Therefore, solving system (32) required the determination of the velocity distribution in the gas phase of the jet. To model the gas phase of the jet, the Euler approach was used, within the

framework of which the axisymmetric flow and the Gaussian velocity distribution in the cross section were assumed (33). The gas dynamics were described by the integral equations of mass balance (34) and momentum balance (35). The mass balance equation takes into account the entrainment of ambient air by the jet. It is the entrainment of air that is the main factor in reducing the velocity of the gas phase of the jet. The right-hand side of the momentum balance equation (35) contains a source term due to the aerodynamic interaction with the droplet phase (36). The combined transformation of the mass and momentum balance equations gave differential equations for the axial velocity (38) and the effective radius of the jet (39).

Although the effect of gravity on the gas phase of the jet is balanced by the Archimedean force, the jet axis is curved due to the gas gaining momentum from water droplets moving downwards under the influence of gravity. As a result of this curvature, the angle of inclination of the jet axis to the horizon is described by the differential equation (40). And the coordinates of the jet axis are given by equations (41), (42). The system of differential equations (38) to (42) under initial conditions (43) to (46) describes the motion of the gas phase of the jet. The 4^{th} order Runge-Kutta method was used for its numerical solution.

Analysis of the results of the numerical solution to the equations of motion of droplets and the gas phase (Fig. 3) reveals that in the drop zone, initially all droplets move along the axis of the jet. At a distance of approximately 10 m horizontally from the fire hydrant, the axial velocity of the gas phase of the jet drops by 3.7 times relative to the initial one (Fig. 4), which increases the aerodynamic resistance of the droplet movement. At the same time, smaller droplets are slowed down more strongly and deviate from the jet axis downwards (Fig. 3). Deviation from the axis leads to an even greater force of aerodynamic resistance due to the lower values of the gas phase velocity at a distance from the axis. As a result, the larger the water droplet, the further it moves along the axis of the gas phase of the jet, reaching a greater height and range.

The dependences shown in Fig. 4 demonstrate that although the axis of the gas phase of the jet undergoes some curvature, it remains close to a straight line. This result differs from [16], in which the axis of the jet is curved, reaching the ground surface together with the droplet stream. The effective radius of the jet increases linearly with increasing distance to the barrel. This is consistent with the known solution for an axisymmetric jet in the absence of a droplet phase.

The randomness of the drop diameter and the dependence of the droplet trajectory on its mass lead to the jet falling to the ground not at a certain distance from the fire barrel but in a range of values (Fig. 5). This result is qualitatively consistent with the jet behavior obtained during the full-scale experiment (Fig. 1), when, as a result of the jet spraying, water falls to the ground over a wide range of distances. According to the tactical and technical characteristics of fire hoses with a diameter of 19 mm, the maximum water supply distance at a head of 60 m is 32 m [23], which is also consistent with the results of the calculations shown in Fig. 5.

An advantage of the constructed model of water jet motion is that it allows us to determine the parameters of water distribution when it is supplied to the fire site depending on the diameter of the barrel, its angle of inclination, and water head. In this case, the mutual influence of the droplet and gas phases of the jet is taken into account.

The proposed model of water jet motion in the air can be used when choosing forces and means for extinguishing a fire or protecting neighboring objects [24]. A limitation of the model is the possibility of its use for fire hydrants designed to supply a continuous water jet, provided that there is no wind.

A disadvantage of our model is that it is based on the stationarity and axisymmetricity of the gas phase of the jet and the integral approach to estimating its momentum. Thus, the prospects for further research are associated with the use of the Navier-Stokes equations to describe motion of the gas phase of the jet.

7. Conclusions

1. The characteristics of the water jet motion in the gravity field in the area of the jet core existence have been determined. It was shown that the length of such an area depends on the diameter of the fire hose and is (4.1 ÷ 7.9) m for fire hoses with a nozzle diameter of (13 ÷ 25) mm at a water head of (20 ÷ 80) m. The jet expansion coefficient with distance from the fire hose was experimentally determined. The value of this coefficient was 0.016. This allowed us to estimate the jet radius at the boundary of the core zone and the drop zone depending on the diameter of the hose. The effective radius of the jet of trapped air at the boundary of these zones was determined, the value of which was (13 ÷ 26) cm. The obtained values are the initial values for modeling the motion of the drop and gas phases of the jet in the drop zone.

2. An equation of motion of the drop phase of the jet has been constructed using the Lagrangian approach, within the framework of which the dynamics of individual drops were considered, described by the equations of motion in three-dimensional space taking into account the forces of aerodynamic resistance and gravity. It is assumed that the distribution of drop diameters obeys the Rosin-Ramler law. A feature of the model is the mutual influence of the drop and gas phases of the jet on the motion of each other. The result of solving the system of drop motion equations is a set of trajectories corresponding to different drops. It is shown that drops of smaller diameter have a shorter range compared to drops of larger diameter. As a result, water falls to the ground not at a certain point but in a certain range. In particular, for a fire hose with a diameter of 19 mm, a feed angle of 35° to the horizon and a water head of (40 ÷ 70) m, the width of the range into which 90% of the water falls was (8.7 ÷ 11) m.

3. An equation of motion of the gas phase of the jet has been constructed, which is based on the equation of mass and momentum balance; it also takes into account the curvature of the axis due to the movement of drops under the action of gravity. The model is based on the assumption of axisymmetric jet and Gaussian velocity distribution in its cross section. It is shown that the radius of the jet increases linearly with increasing distance to the fire hydrant, and the velocity decreases inversely proportional to this distance. The motion of the gas phase of the jet together with

the drops reduces aerodynamic resistance and increases the range of the jet. The calculated maximum range of water supply by a hydrant with a diameter of 19 mm, located at an angle of 35° to the horizon, is (30.2 ÷ 38.2) m for a head of (40 ÷ 70) m, which corresponds to the tactical and technical characteristics of actual fire hydrants.

Conflicts of interest

The authors declare that they have no conflicts of interest in relation to the current study, including financial, personal, authorship, or any other, that could affect the study, as well as the results reported in this paper.

Funding

The study was conducted without financial support.

Data availability

The data will be provided upon reasonable request.

Use of artificial intelligence

The authors confirm that they did not use artificial intelligence technologies when creating the current work.

References

1. Rahman, F. S., Tannous, W. K., Avsar, G., Agho, K. E., Ghassempour, N., Harvey, L. A. (2023). Economic Costs of Residential Fires: A Systematic Review. Fire, 6 (10), 399. https://doi.org/10.3390/fire6100399
2. Kawade, A. U., Kawade, P. A., Kaware, A. P., Kkulthe, A. A., Amune, A. C. (2022). Smart Fire Fighting Robot. World Journal of Advanced Engineering Technology and Sciences, 7 (2), 157–162. https://doi.org/10.30574/wjaets.2022.7.2.0137
3. Abramov, Y., Basmanov, O., Krivtsova, V., Khyzhnyak, A. (2020). Estimating the influence of the wind exposure on the motion of an extinguishing substance. EUREKA: Physics and Engineering, 5, 51–59. https://doi.org/10.21303/2461-4262.2020.001400
4. Etzold, M., Deswal, A., Chen, L., Durst, F. (2018). Break-up length of liquid jets produced by short nozzles. International Journal of Multiphase Flow, 99, 397–407. https://doi.org/10.1016/j.ijmultiphaseflow.2017.11.006
5. Fan, Q., Deng, Q., Liu, Q. (2024). Research and application on modeling and landing point prediction technology for water jet trajectory of fire trucks under large-scale scenarios. Scientific Reports, 14 (1). https://doi.org/10.1038/s41598-024-72476-y
6. Hou, X., Cao, Y., Mao, W., Wang, Z., Yuan, J. (2021). Models for Predicting the Jet Trajectory and Intensity Drop Point of Fire Monitors. Fluid Dynamics & Materials Processing, 17 (5), 859–869. https://doi.org/10.32604/fdmp.2021.015967
7. Sallam, K. A., Dai, Z., Faeth, G. M. (2002). Liquid breakup at the surface of turbulent round liquid jets in still gases. International Journal of Multiphase Flow, 28 (3), 427–449. https://doi.org/10.1016/s0301-9322(01)00067-2
8. Rezayat, S., Farshchi, M., Berrocal, E. (2021). High-speed imaging database of water jet disintegration Part II: Temporal analysis of the primary breakup. International Journal of Multiphase Flow, 145, 103807. https://doi.org/10.1016/j.ijmultiphaseflow.2021.103807
9. Liu, X., Wang, J., Li, B., Li, W. (2018). Experimental study on jet flow characteristics of fire water monitor. The Journal of Engineering, 2019 (13), 150–154. https://doi.org/10.1049/joe.2018.8950
10. Trettel, B. (2020). Reevaluating the jet breakup regime diagram. Atomization and Sprays, 30 (7), 517–556. https://doi.org/10.1615/atomizspr.2020033171
11. Trettel, B., Ezekoye, O. A. (2015). Theoretical Range and Trajectory of a Water Jet. Volume 7A: Fluids Engineering Systems and Technologies. https://doi.org/10.1115/imece2015-52103
12. Zhu, J., Li, W., Lin, D., Zhao, G. (2018). Study on Water Jet Trajectory Model of Fire Monitor Based on Simulation and Experiment. Fire Technology, 55 (3), 773–787. https://doi.org/10.1007/s10694-018-0804-1
13. Kooij, S., Sijs, R., Denn, M. M., Villermaux, E., Bonn, D. (2018). What Determines the Drop Size in Sprays? Physical Review X, 8 (3). https://doi.org/10.1103/physrevx.8.031019
14. Privitera, S., Manetto, G., Pascuzzi, S., Pessina, D., Cerruto, E. (2023). Drop Size Measurement Techniques for Agricultural Sprays:A State-of-The-Art Review. Agronomy, 13 (3), 678. https://doi.org/10.3390/agronomy13030678
15. Salyers B. E. (2010). Spray Characteristics From Fire Hose Nozzles. University of Maryland. Available at: https://drum.lib.umd.edu/items/bd81aff2-327f-4cfe-8047-58e5515c0396
16. Valencia, A., Zheng, Y., Marshall, A. W. (2021). A Model for Predicting the Trajectory and Structure of Firefighting Hose Streams. Fire Technology, 58 (2), 793–815. https://doi.org/10.1007/s10694-021-01175-1
17. Fan, X., Wang, J., Zhao, F., Li, J., Yang, T. (2018). Eulerian–Lagrangian method for liquid jet atomization in supersonic crossflow using statistical injection model. Advances in Mechanical Engineering, 10 (2). https://doi.org/10.1177/1687814018761295
18. Semko, A., Rusanova, O., Kazak, O., Beskrovnaya, M., Vinogradov, S., Gricina, I. (2015). The use of pulsed high-speed liquid jet for putting out gas blow-out. The International Journal of Multiphysics, 9 (1), 9–20. https://doi.org/10.1260/1750-9548.9.1.9
19. Zhang, C., Zhang, R., Dai, Z., He, B., Yao, Y. (2019). Prediction model for the water jet falling point in fire extinguishing based on a GA-BP neural network. PLOS ONE, 14 (9), e0221729. https://doi.org/10.1371/journal.pone.0221729

20. Cheng, H., Zhu, J., Wang, S., Yan, K., Wang, H. (2024). A Study on Predicting the Deviation of Jet Trajectory Falling Point under the Influence of Random Wind. Sensors, 24 (11), 3463. https://doi.org/10.3390/s24113463
21. Lin, Y., Ji, W., He, H., Chen, Y. (2021). Two-Stage Water Jet Landing Point Prediction Model for Intelligent Water Shooting Robot. Sensors, 21 (8), 2704. https://doi.org/10.3390/s21082704
22. Vambol, S., Vambol, V., Abees Hmood Al-Khalidy, K. (2019). Experimental study of the effectiveness of water-air suspension to prevent an explosion. Journal of Physics: Conference Series, 1294 (7), 072009. https://doi.org/10.1088/1742-6596/1294/7/072009
23. EN 15182-2. Portable equipment for projecting extinguishing agents supplied by firefighting pumps – Hand-held branchpipes for fire service use. Part 2: Combination branchpipes PN 16. Available at: https://www.normsplash.com/FreeDownload/115458135/DIN-EN-15182-2-2019-en.PDF
24. Abramov, Y. A., Basmanov, O. E., Salamov, J., Mikhayluk, A. A. (2018). Model of thermal effect of fire within a dike on the oil tank. Naukovyi Visnyk Natsionalnoho Hirnychoho Universytetu, 2, 95–101. https://doi.org/10.29202/nvngu/2018-2/12